Original Article

A novel biomarker NIFK-AS1 promotes hepatocellular carcinoma cell cycle progression through interaction with *SRSF10*

Huibin Song[1], Wenjing Li[2], Sixuan Guo[3], Zhentao He[4], Shi Liu[4], Yongsheng Duo[5]

[1]Department of Emergency Surgery, The Third Affiliated Hospital of Qiqihar Medical University, Qiqihar, China; [2]Pharmacy School, Qiqihar Medical University, Qiqihar, China; [3]The Second Clinical College, Medical College of Nanchang University, Nanchang, China; [4]Department of General Surgery, The Third Affiliated Hospital of Qiqihar Medical University, Qiqihar, China; [5]Department of Vascular Burn Surgery, The Third Affiliated Hospital of Qiqihar Medical University, Qiqihar, China

Contributions: (I) Conception and design: Y Duo, W Li, H Song; (II) Administrative support: S Liu; (III) Provision of study materials or patients: Z He, S Liu; (IV) Collection and assembly of data: H Song; (V) Data analysis and interpretation: S Guo; (VI) Manuscript writing: All authors; (VII) Final approval of manuscript: All authors.

Correspondence to: Yongsheng Duo. Department of Vascular Burn Surgery, The Third Affiliated Hospital of Qiqihar Medical University, No. 27, Taishun Street, Tiefeng District, Qiqihar 161000, China. Email: Duoyongsheng210905@163.com.

Background: Hepatocellular carcinoma (HCC) is one of the most common carcinomas all over the world, with high mortality and low survival rate. Notably, many studies have showed that a variety of molecules play vital roles in the progression of HCC. Therefore, it is urgent to find reliable biomarkers to diagnose HCC and developing novel strategies are required for the effective treatment of patients with HCC.

Methods: This study obtained an HCC cohort from The Cancer Genome Atlas (TCGA). For prognostic analysis, the TCGA cohort was grouped according to different median boundaries. The key module associated with HCC was adopted by Weighted Gene Co-expression Network analysis (WGCNA). We also analyzed the survival ability, functional enrichment, and potential binding proteins of key lncRNAs. The expression of hub lncRNAs in HCC tissues and cell lines was detected by reverse transcription-quantitative polymerase chain reaction (RT-qPCR). Cell Counting Kit-8 (CCK-8) and flow cytometry were applied to detect the cell proliferation, apoptosis, and cell cycle. The interaction between *NIFK-AS1* and SRSF1 was examined using an RNA pull-down assay.

Results: The green module is the key module in HCC. *NIFK-AS1* was highly expressed in HCC tissues and correlated with a poor prognosis in HCC patients (P=0.008). *NIFK-AS1* was also significantly associated with cell mitosis, the cell cycle, and other biological processes. *NIFK-AS1* deletion prevented cell proliferation, induced apoptosis, caused G2/M arrest, and affected cell cycle progression. RNA pull-down validated the *NIFK-AS1/SRSF10* interaction. The overexpression of *NIFK-AS1* was sufficient to rescue the growth of *SRSF10* knockdown HepG2 cells.

Conclusions: This study suggested that *NIFK-AS1* promotes HCC cell cycle progression through interaction with *SRSF10* and its findings provide new insights into therapeutic targets for HCC.

Keywords: NIFK antisense RNA 1 (*NIFK-AS1*); hepatocellular carcinoma (HCC); *SRSF10*; long non-coding RNA (lncRNA)

Submitted Jul 04, 2022. Accepted for publication Aug 10, 2022.
doi: 10.21037/jgo-22-705
View this article at: https://dx.doi.org/10.21037/jgo-22-705

Introduction

Hepatocellular carcinoma (HCC) is the most common primary malignant tumor of the liver, accounting for 80–90% of primary liver cancers (1), and most patients are already in an advanced stage at first diagnosis. Surgical resection, liver transplantation, chemotherapy, radiotherapy, and tumor ablation are potential treatment methods (2-4). Currently, ultrasonography (US) tests are recommended by all guidelines with or without serum alpha-fetoprotein (AFP) assessments for early HCC detection. Cross-sectional imaging techniques are further recommended for liver nodules ≥1 cm. Despite the significant progress in tumor diagnosis and treatment, the 5-year survival of most patients remains very low (5). Additionally, particularly in the early stages of the disease, the sensitivity and specificity of the clinical tests employed for HCC diagnosis remain inadequate. Therefore, further study regarding the potential mechanism of the biological process of liver cancer progression is urgently needed.

Long non-coding RNA (lncRNA) are RNA molecules larger than 200 nucleotides in length that cannot encode proteins (6). An increasing number of studies have shown that lncRNAs are related to tumor generation, progression, metastasis, and prognosis (7,8). Numerous lncRNAs are key molecules regulating the biological processes in cancer, such as the individual cell cycle as well as cell growth, proliferation, migration, invasion, and apoptosis (9-11). Some lncRNAs may potentially be utilized as diagnostic biomarkers and therapeutic bio-targets for HCC treatment (12), and are influential in colorectal cancer (13), pancreatic ductal adenocarcinoma (14), breast cancer (15), and the occurrence of prostate cancer (16).

A previous study reported that NIFK antisense RNA 1 (*NIFK-AS1*) inhibits the polarization of M2 macrophages by inhibiting microRNA-146a (miR-146a). As a result, the proliferation, migration, and invasion of cells of endometrial cancer are reduced (17). Also, Zhang *et al.* found that *NIFK-AS1* can be considered a diagnostic biomarker and target for different types of breast cancer (18). However, the clinical significance of *NIFK-AS1* in HCC remains unclear.

Our study aims to determine the underlying clinical importance of *NIFK-AS1* in patients with early-stage HCC, including its diagnostic value, functional underlying mechanism, as well as the binding proteins for targeted therapy. We present the following article in accordance with the TRIPOD and MDAR reporting checklists (available at https://jgo.amegroups.com/article/view/10.21037/jgo-22-705/rc).

Methods

Data collection

The clinical characteristics and RNA Sequencing (RNA-seq) expression data of HCC patients and healthy individuals were obtained from The Cancer Genome Atlas (TCGA, https://portal.gdc.cancer.gov/), which includes clinically-relevant information such as age, gender, pathology M, pathology N, pathology T, histological grade, mutation count, and genomic changes. In addition, we searched the Gene Expression Omnibus (GEO, http://www.ncbi.nlm.nih.gov/geo/) for eligible HCC datasets. All datasets adopted in this study were downloaded and manipulated in accordance with the guidelines issued by relevant publication agencies.

Patient and tissue samples

All primary HCC tissues and adjacent healthy tissues were collected from clinically-treated patients who underwent vascular burn surgical procedures performed at the Third Affiliated Hospital of Qiqihar Medical University from January 2019 to May 2021. The study was conducted in accordance with the Declaration of Helsinki (as revised in 2013) and was approved by the institutional ethics board of the Third Affiliated Hospital of Qiqihar Medical University (No. 2018LL-21). Informed consent was obtained from the included patients.

TCGA data was used to perform weighted gene co-expression network analysis (WGCNA)

TCGA data with detailed clinical information is crucial for WGCNA, which would allow us to link the apparent and hidden modular characteristic genes with the clinical information obtained from HCC patients. Using TCGA data, we established a data matrix of gene expression and applied the "WGCNA" function in the R/Bioconductor software (https://www.bioconductor.org/) to select differentially-expressed lncRNA (DEL) as the computer input set of information adopted for the subsequent construction of the WGCNA network. Before choosing the most optimal soft threshold power to implement the network with scale-free quality, we adopted the hierarchical clustering method of sample processing to identify and oversee abnormal and contaminated samples.

Next, we utilized an adjacent matrix, topological overlap matrix (TOM) and 1-TOM, as our analyzing scheme. We completed the whole-gene tree diagram and the process of module identification through dynamic tree cutting, and then set the minimum size of our calculated module to 100. Finally, the module eigengenes method was employed; we merged genes with characteristic attributes and highly similar modules with a different degree of <0.25. We discovered the interconnection between genes with characteristic attributes from our module and the clinically demonstrated phenotype that belongs to HCC through dynamic tree cutting to identify modules that are related to the clinical manifestations of HCC.

Survival analysis of HCC DELs and hub genes

We utilized univariate Cox regression analysis (UCRA) to investigate the potential correlation between patients' HCC expression levels and DELs. We selected the gene with the lowest P value as the central lncRNA for further analysis and then distinguished the high expression level group from the low expression level group using the median value expression demonstrated by the hub lncRNA. Next, we adopted the Kaplan-Meier (KM) and Log-Rank (LR) tests to clarify the differences in prognostic results between groups with different expressions of hub lncRNA. The time-dependent receiver operating characteristic (ROC) curve was utilized to further evaluate the expression of the hub lncRNA for the prediction of HCC prognosis. This step was carried out using the R software "survival" package.

In addition, we also established a clinically applicable survival prediction method for HCC patients using a renounced multivariate Cox proportional hazard regression (MCPHR) model. A nomogram was utilized to evaluate the key lncRNA expression level and clinical parameters for HCC prognosis. The above steps were performed using the "rms" package in the R software. A final chart of the calibrated result was utilized to visually display the nomogram and its performance.

Functional and optimal enrichment of jointly-expressed genes from the hub lncRNA

It is well known that in the post-transcriptional phase, the main function of lncRNA is mainly achieved by regulating the expression levels of PCGs. Thus, there exists a strong potential connection between a designated lncRNA and a lncRNA-regulated PCG. In this study, we utilized "r", the Pearson correlation coefficient, to identify and distinguish PCGs that are generally connected to the key lncRNA, and those with $P<0.05$ and $|r|>0.45$ were considered to be associated with lncRNA.

To better anticipate the potential biological regulatory function of the key lncRNA and identify the significantly-enriched Gene Ontology (GO) and Kyoto Encyclopedia of Genes and Genomes (KEGG) terms, we used functional enrichment analysis (FEA) on the lncRNA-related PCGs that demonstrated co-expression abilities.

Cell culture and transfection

The cell lines (HCC-9204, A549, Hep3B, HepG2, PLC, LM3, Huh7, and human normal hepatocyte LO2) were all acquired from the Shanghai Institute of Life Sciences. We cultivated all of the aforementioned cell lines according to ATCC's protocols. The cell lines were supplemented with 10% fetal bovine serum (FBS) containing penicillin (100 μg/mL) and streptomycin (100 mg/mL), and then cultured in humid air at a temperature of 37 ℃ and 5% CO_2 humidity. We also introduced HepG2 cells into a six-well plate with a container density of 1 by 105 cells per well and then introduced short-hairpin RNAs with lentivirus-expressing capability directly against the purchased human *NIFK-AS1*—short hairpin(sh)-*NIFK-AS1* and sh-negative control (NC). The abovementioned items were all purchased from GenePharma (Shanghai). The lentivirus that directly expresses human SRSF10 (sh-SRSF10) was also purchased from the same manufacturer. The full-length complementary DNA (cDNA) of human NIFK-AS1 was also prepared by GenePharma Shanghai Branch Company and cloned into a pCDNA3.1 expression vector. We also utilized Lipofectamine 2000 (Invitrogen, USA) for the transfection of pcDNA-*NIFK-AS1*, sh-*NIFK-AS1*, and the negative control according to the manufacturer's instructions. After 24 hours of transfection, we collected the cells and performed the following experiments.

Western blot RNA extraction analysis and quantitative PCR in real time

We used TRIzol reagent (Life Technologies, USA) to extract the total RNA from cell and tissue samples. Briefly, we followed the manufacturer's instructions and protocol, and then utilized a cDNA First-Strand synthesis kit (Tiangen Biotechnology, Beijing Branch) to reverse transcribe a total of 1 μg RNA into cDNA. Relative

quantification of the *NIFK-AS1* expression level was carried out using the ABI 7500 real-time PCR system (Applied Biosystems, Carlsbad, CA, USA). Next, we performed $2^{-\Delta\Delta Ct}$ calculation using the MiRcute miRNA qPCR detection kit (Tiangen Biotech). For better experimental results, we used glyceraldehyde-3phosphate dehydrogenase (GAPDH) as a control.

Cell proliferation, apoptosis, and cell cycle measurement

After 24 hours of transfection, we collected the cells and seeded them in 96-well plates at $5*10^3$ cells/well. All cells were incubated overnight. After 48, 72, and 96 hours of transfection, we measured the cell proliferation using Cell Counting Kit-8 (CCK-8, Roche Applied Science, USA). To determine the distribution of cell cycles by flow cytometry, we seeded the cells in six-well plates at a density of 5×10^5/well. The experimental and control groups were assigned three wells each. Following incubation overnight, we transfected the experimental and control groups of HCC cells with sh-NC and sh-*NIFK-AS1*, respectively. After 48 hours of transfection, we stained the cells in the dark with a 0.025 mg/mL propidium iodide (PI) and 0.1% (v/v) Triton X-100 staining solution for DNA processing over a period of 30 minutes. Thereafter, we used an Attune™ flow cytometer (Thermo Fisher Scientific, USA) to analyze the cell cycle distribution.

To determine the apoptotic rate by flow cytometry, we collected the cells 48 hours after transfection. Next, we washed those cells with phosphate buffer saline (PBS) twice. Finally, we double-labeled these experimental cell groups with eBioscience-PI and Annexin V-FluoresceinIsothiocyanate (FITC) as described by the manufacturer. The experimental cell groups were then analyzed using the Attune™ flow cytometer.

Bioinformatics prediction

The binding tendency of the hub lncRNA and potential binding protein pairs were estimated using the algorithm provided by catRAPID and the lncRNA-protein interaction prediction results. Subsequently, we utilized the catRAPID omics, feature, and fragment modules in catRAPID to better predict the RNA target protein binding region and the correlation between the experimental central lncRNA and the target protein. The computer-generated result and the predicted relationship between the target protein and the central lncRNA were utilized to calculate the predictive result.

Pull-down assay of experimental RNA

We adopted the Pierce Magnetic RNA-Protein Pull-Down Kit (Thermo Fisher) to examine the interaction between *NIFK-AS1* and *SRSF10* through RNA pull-down, according to the manufacturer's instructions. Briefly, the examined HepG2 experimental cells were then washed for 30 minutes with cold PBS and lysed. This procedure was performed in radioimmunoprecipitation buffer at 4 ℃. Subsequently, the protein extract of HepG2 cells was mixed with 50 pmol of biotinylated *NIFK-AS1*. The protein extract was then incubated with magnetic beads (Life Technologies) containing 50 μL streptavidin Sepharose for 1 hour, and the temperature was controlled constantly at 4 ℃. After eluting the relevant complex of RNA and protein, which contains biotin elution buffer, we boiled it in a buffer with Sodium dodecyl sulfate (SDS) for 10 minutes. Next, the protein level of *SRSF10* retrieved by western blotting was detected. Subsequently, the membrane was blocked with 5% skim milk, and the primary antibodies blot was incubated against *SRSF10* (ab161147, Abcam, Cambridge, UK) and GAPDH (ab8245, Abcam, Cambridge, UK), respectively. The blot was then incubated with the appropriate secondary antibody. We then used the Pierce ECL Western Blotting Substrate (Santa Cruz Biotechnology, USA) to observe and analyze the immune response bands. Finally, we normalized the experimental results to GAPDH for internal reference.

Statistical analysis

We utilized R (version 3.6.3) (https://cran.r-project.org/bin/windows/base/old/), GraphPad Prism 8 (graphpad-prism.cn), and SPSS 23 (https://www.onlinedown.net/soft/1225981.htm) software to analyze the data and draw graphs. We performed a two-tailed student's *t*-test to better identify the statistical differences between the control and experimental groups. The Pearson correlation test was adopted to assess the strength of the association between continuous variables. We then utilized univariate and multivariate Cox (UMC) regression to identify various independent risk factors. To better evaluate the sensitivity and specificity of the hub lncRNA in diagnosing HCC, we performed an experimental ROC curve analysis using "medcalc" software (MedCalc Software Ltd., Ostend, Belgium). All P values were double-sided, and $P<0.05$ was considered to indicate statistical significance.

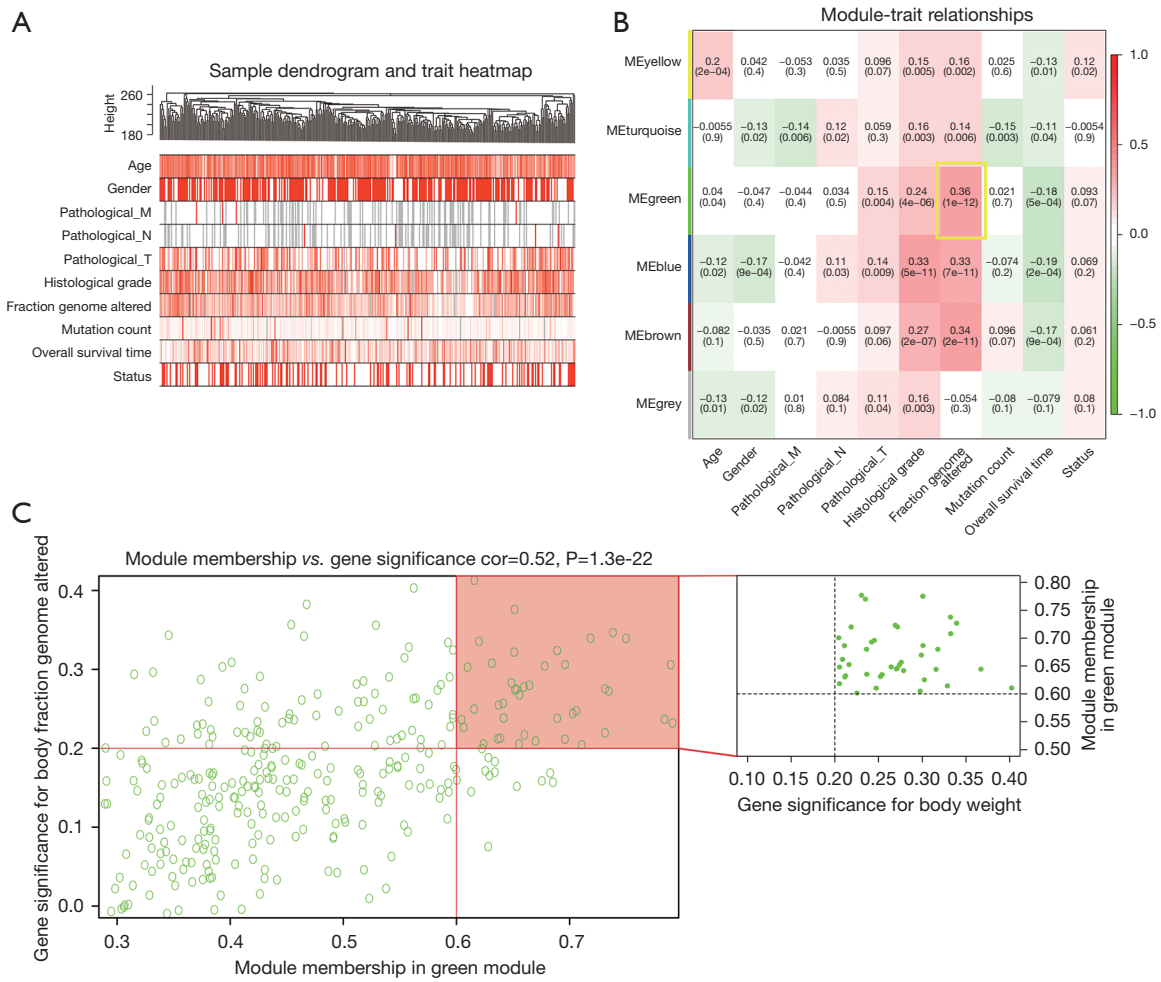

Figure 1 WGCNA construction and DEL recognition. (A) HCC processing of samples from TCGA data. The clinical features of some genomic changes are shown at the bottom (Age, Gender, Pathological_M, Pathological_N, Pathological_T, Histological grade, Fraction genome altered, Mutation count, Overall survival time, Status). (B) The module-partial genome relationship changes were analyzed using the (r) - PCC, and the P value is shown in the parentheses. (C) GS/MM scatter plot, where the genome of the HCC patient has been changed. ME, module eigengene; WGCNA, weighted gene co-expression network analysis; DEL, differentially expressed lncRNA; HCD, hierarchical clustering dendrogram; TCGA, The Cancer Genome Atlas; PCC, Pearson Correlation Coefficient; GS/MM, Gene Significance/Module Membership; HCC, hepatocellular carcinoma.

Results

Weighted gene co-expression network analysis (WGCNA) lncRNA scanning

This study included 369 HCC patients and 50 healthy samples. Among the HCC patients, we were enrolled a total of 365 samples, containing survival data in WGCNA (*Figure 1A*). Pathological diagnostic criteria of HCC was that the specimen obtained during surgery or the liver puncture specimen was identified as HCC after pathological examination. The case group with negative diagnosis of pathological section and the control group with positive diagnosis. We set scale-free R^2=0.900 and β=4 as the soft threshold for the scale-free network (Figure S1A-S1D). After excluding the gray modules, we adopted the merged dynamic tree cut to identify five gene co-expression modules (Figure S1E). The heat map plotted the TOM among 400 selected genes in the analysis, which revealed that every module was an independent validation to each other (Figure S1F).

Table 1 Top 10 dysregulated lncRNAs

Gene	P value	Chi	HR
NIFK-AS1	0.00060	11.76626	1.84134
SNHG20	0.00064	11.66536	1.83709
GIHCG	0.00112	10.61087	1.78278
Z95115.1	0.00238	9.23009	1.71497
AL050341.2	0.00427	8.16553	1.66203
AC010864.1	0.00715	7.23418	1.60575
STK24-AS1	0.00837	6.95276	1.59472
AL592435.1	0.01139	6.40277	1.56582
SNHG21	0.01177	6.34587	1.56239
AC074117.1	0.01332	6.12643	1.55108

HR, hazard rate.

We drew scatter plots of Gene Significance (GS) *vs.* Module Membership (MM) in the green module with altered genome fractions of HCC patients (correlation =0.52, P=1.3e-22), elaborating that 40 lncRNAs were the genes under the condition of MM >0.60 and GS <0.20 (*Figure 1B*,*1C*).

Identification of NIFK-AS1 as a prognostic factor for HCC

We performed a UCRA to study the correlation and interconnection between HCC patient survival and the expression levels of the 40 lncRNAs in the green module. *NIFK-AS1* is considered to be the key gene, with the lowest P and highest hazard rate (HR) values (*Table 1*). In addition, survival analysis of the different *NIFK-AS1* expression groups was also performed. Through our experiments, we found that high *NIFK-AS1* expression significantly increased the risk of cancer-related death (*Figure 2A*,*2B*). The high expression of *NIFK-AS1* is somehow connected to the poor prognostic results of HCC patients (P=6e-04, *Figure 2C*).

The clinical information of HCC patients was analyzed by univariate Cox analysis, and the results showed that the survival rate of patients was significantly correlated with Pathological_M (P=0.01) and Pathological_T (P=5.0E-07) (*Table 2*).

Next, we combined these factors with *NIFK-AS1* expression for multivariate Cox analysis (*Figure 2D*). The nomogram indicated that the expression level of NIFK-AS1 significantly impacted the progress and diagnosis of HCC patients, which were second only to pathological T (*Figure 2E*). Survival analysis of the combined effect showed that combining *NIFK-AS1* with clinical parameters could increase the accuracy and possibility of a successful prognostic prediction. The calibration chart showed that the resulting nomogram performed well (*Figure 2F-2H*).

NIFK-AS1 is a biomarker for HCC diagnosis

We also explored the potential significance of NIFK-AS1 in the detection of HCC and determined the NIFK-AS1 expression level. We decided to examine the NIFK-AS1 expression level in adjacent non-tumor tissues and 20 pairs of HCC tissues using the RT-qPCR method and then compared these results with healthy, adjacent, non-tumor tissues. The experimental results showed that the NIFK-AS1 expression level in HCC tissues was significantly higher than that in healthy tissues (P<0.05, *Figure 3A*).

We then sequentially tested the *NIFK-AS1* expression indicator in LO2, a normal human hepatocyte, and seven HCC cell lines (HCC-9204, A549, Hep3B, HepG2, PLC, LM3, Huh7). As shown in *Figure 3B*, compared with the normal human liver cell lines, *NIFK-AS1* was up-regulated and the indexes were higher in HCC cell lines. In summary, our experimental data demonstrated that the level of NIFK-AS1 is up-regulated in HCC.

Next, we performed a ROC curve analysis to calculate and assess the sensitivity and specificity of *NIFK-AS1* in the diagnosis of HCC. *NIFK-AS1* is a favorable indicator for diagnosing HCC in TCGA data, and its AUC value is 0.885 (*Figure 3C*). To verify the diagnostic significance of NIFK-AS1, we selected the GSE41804 dataset, which included 20 HCC patients and 20 healthy individuals (*Figure 3C*). Subsequently, we modeled the logistic regression to further evaluate the diagnostic effectiveness of *NIFK-AS1* for HCC (*Figure 3D*). After constructing the confusion matrix, the average values of accuracy, accuracy, recall, F measurement, and AUC were 0.886, 0.901, 0.978, 0.938, and 0.885, respectively (*Figure 3E*). These results indicate that NIFK-AS1 exhibits good performance and can distinguish HCC samples from normal controls.

Exploration of the related molecular mechanisms of NIFK-AS1

According to our experimental results and the median expression of the performance of *NIFK-AS1*, we categorized PCGs into low and high NIFK-AS1 level groups. We

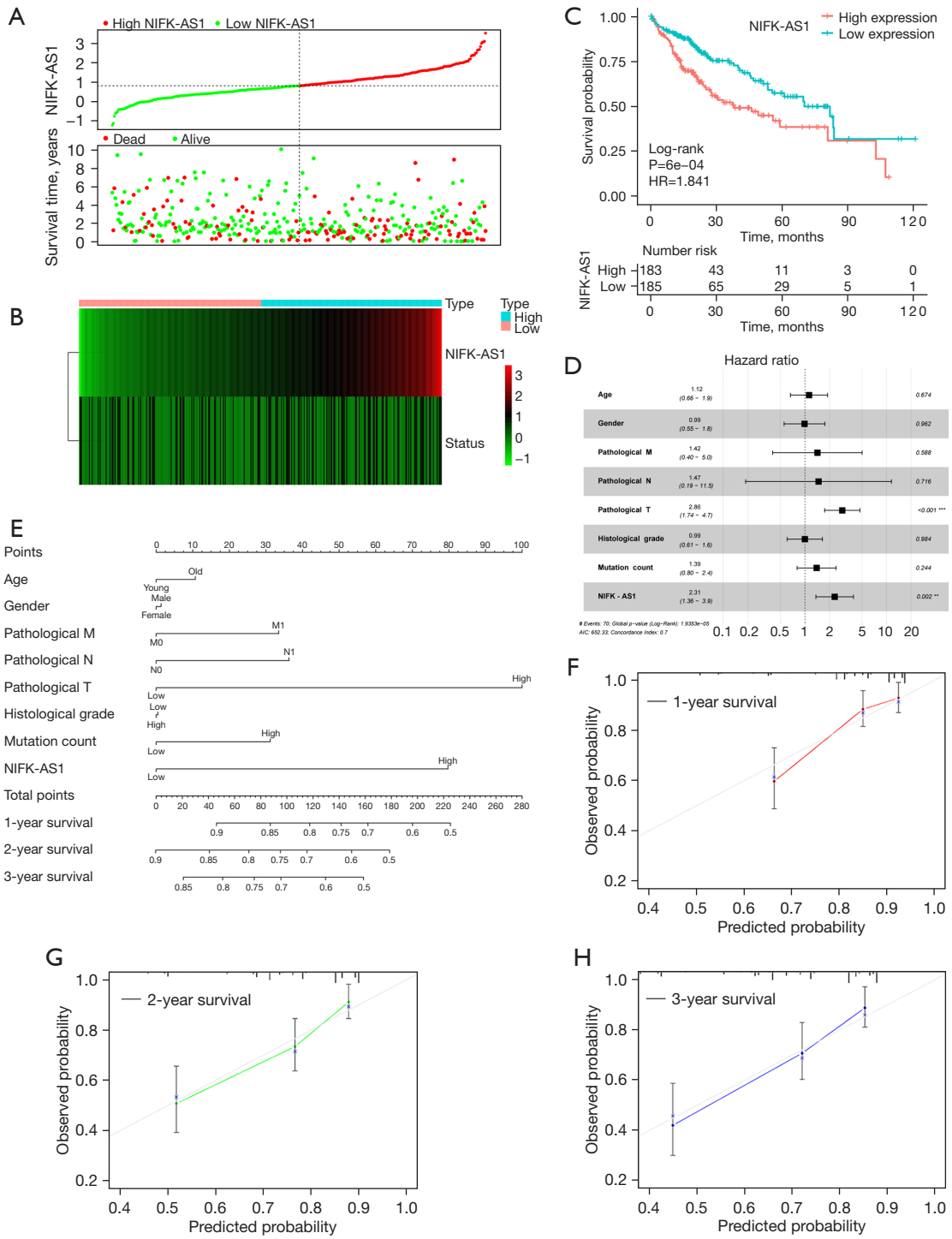

Figure 2 Survival analysis of *NIFK-AS1* expression in HCC patients and statistical analysis of *NIFK-AS1* and clinical parameters. (A,B) Scatter plots and heat maps showing the expression of *NIFK-AS1* and the survival time of HCC patients. (C) Survival curve between the high and low *NIFK-AS1* gene expression groups. (D) Multivariate analysis of *NIFK-AS1* and clinical information. (E) *NIFK-AS1* gene nomogram and the practical parameters in TCGA HCC cohort during clinical practice. (F-H) Calibration chart showing the 1-, 2-, and 3-year survival. **, P<0.01; ***, P<0.001. *NIFK-AS1*, NIFK antisense RNA 1; HCC, hepatocellular carcinoma; TCGA, The Cancer Genome Atlas.

Table 2 Univariate Cox analysis of the clinical information of HCC patients

Variables	Events that occurred versus the total value (n=226)	Experimental MST in days	HR index, 95% CI	Value of Log rank, P
Age (years)				0.4
Young (≤50)	35/127	579.0	1	
Old (>50)	35/99	578.4	1.24 (0.78–1.99)	
Gender				0.4
Male	44/157	577.5	1	
Female	26/69	585.3	1.23 (0.75–2.00)	
Pathological_M				0.01
M0	67/222	579.0	1	
M1	3/4	342.0	4.05 (1.27–12.94)	
Pathological_N				0.8
N0	69/223	579.0	1	
N1	1/3	689.4	1.28 (0.18–9.22)	
Pathological T				5.0E-07
Low	36/163	577.5	1	
High	34/63	579.0	3.15 (1.96–5.05)	
Histological Grade				1
Low	40/128	578.4	1	
High	30/98	585.3	1.00 (0.62–1.61)	
Mutation count				0.3
Low	33/114	579.0	1	
High	37/112	576.6	1.30 (0.81–2.08)	

HCC, hepatocellular carcinoma; MST, median survival time; HR, hazard rate; CI, confidence interval.

selected 850 obtained PCGs, including 196 down-regulated and 654 up-regulated candidates (*Figure 4A*, Table S1). Pathway evaluation revealed that these PCGs were related to the mitotic cell cycle process, organelle fission, nuclear division, and chromosome segregation (Table S2). Moreover, KEGG analysis showed that these PCGs were significantly related to the cell cycle and chemical carcinogenesis (*Figure 4B*,*4C*).

NIFK-AS1 knockdown inhibited HCC cell proliferation, induced apoptosis, and affected the cell cycle in vitro

To comprehensively understand the mechanism of NIFK-AS1 behavior in HCC at the molecular level, we applied the gene set enrichment analysis (GSEA) method with c5 as the reference set to analyze the complete genome-wide t value between different NIFK-AS1 expression levels. Our experimental results showed that the processes of homologous recombination, spliceosome, DNA replication, mismatch repair, nucleotide excision repair, and the cell cycle were interconnected with the high NIFK-AS1 expression HCC group (Figure S2A-S2G).

To clarify the biochemical effect of NIFK-AS1 on HCC in terms of the cell cycle, we selected HepG2 with the highest expression of *NIFK-AS1* as the model for subsequent experiments. Then *NIFK-AS1* was knockdown in HepG2 and the silencing effect was examined by RT-qPCR. As shown in *Figure 5A*, the messenger RNA (mRNA) expression level of *NIFK-AS1* was markedly diminished following transfection with the specific-sh-*NIFK-AS1* (P<0.001). In particular, sh-

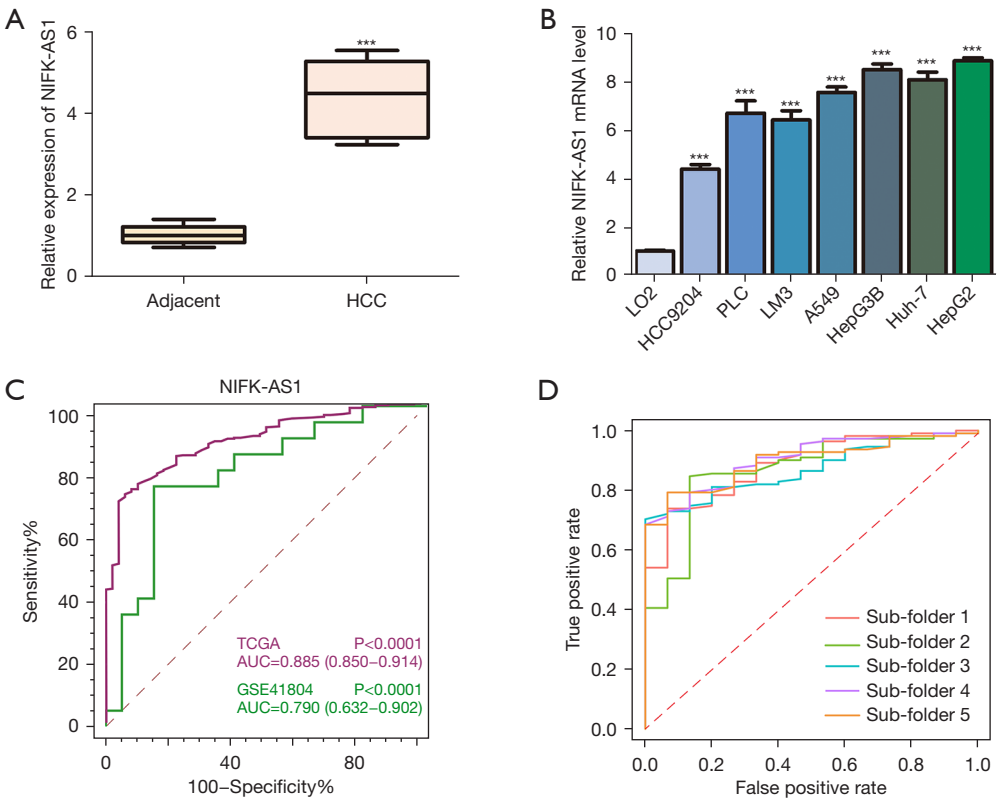

E

	Accuracy	Precision	Recall	F measure	AUC
Sub-folder 1	0.897	0.902	0.991	0.944	0.886
Sub-folder 2	0.881	0.893	982	0.936	0.867
Sub-folder 3	0.881	0.907	0.964	0.934	0.871
Sub-folder 4	0.889	0.894	0.991	0.94	0.904
Sub-folder 5	0.881	0.907	0.964	0.934	0.897
Average	0.886	0.901	0.978	0.938	0.885

Figure 3 Up-regulation of the *NIFK-AS1* gene in HCC is a biomarker for HCC diagnosis. (A) The *NIFK-AS1* gene is highly expressed in HCC-derived tissues. RNA was isolated from adjacent healthy tissues for RT-qPCR analysis (total 20 pairs). (B) Up-regulation of the *NIFK-AS1* gene in HCC cell lines. The three tiers demonstrated represent, ***, P<0.001. (C) The ROC curve was adopted to evaluate the sensitivity and specificity of *NIFK-AS1* gene expression. To determine whether such expression could be adopted as a diagnostic biomarker for the diagnosis of HCC, we acquired data from databases of TCGA and the GSE41804 data. (D) The *NIFK-AS1* gene ROC curve demonstrating the process and results of five-fold cross-validation and the calculated evaluation index of each fold. (E) The evaluation index for each fold. All data mentioned above are expressed as mean ± standard deviation (SD). *NIFK-AS1*, NIFK antisense RNA 1; HCC, hepatocellular carcinoma; RT-qPCR, reverse transcription polymerase chain reaction; TCGA, The Cancer Genome Atlas; ROC, receiver operating characteristic; AUC, area under curve.

NIFK-AS1-#1 and -#2 were more significantly reduced and were selected for subsequent experiments.

For the initial assessment of the possibility of NIFK-AS1 as a target of HCC-related therapy, our research analyzed the consequence of *NIFK-AS1* knockdown on the proliferation of cells *in vitro*. CCK-8 assays revealed a profound decrease in cell proliferation after *NIFK-AS1* knockdown (*Figure 5B*). Subsequently, we examined whether the inhibitory effects of *NIFK-AS1* knockdown may be at least in part attributable to the elevated cell death.

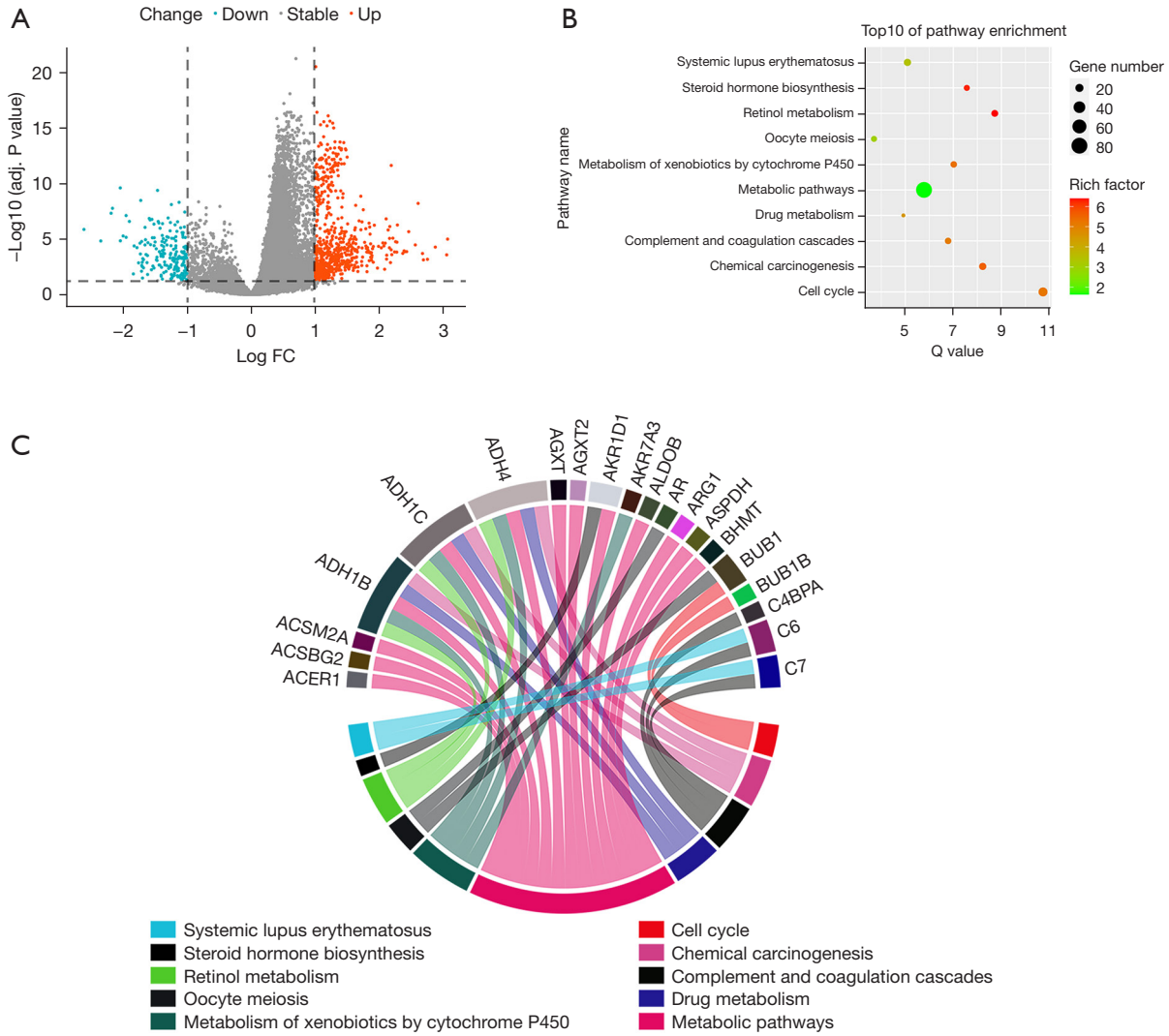

Figure 4 Identification and functional annotation of *NIFK-AS1*-related differentially-expressed PCGs. (A) VP of PCGs in the high and low *NIFK-AS1* gene expression groups in HCC tumor tissue. (B) Bubble chart of the top 10 significant enrichment pathways. (C) Through the KEGG pathway, the enrichment analysis of KEGG pathway enrichment analysis showed that PCGs were significantly related to the cell cycle *NIFK-AS1*, NIFK antisense RNA 1; VP, volcano plot; PCG, Protein-Coding Gene; HCC, hepatocellular carcinoma; ROC, receiver operating characteristic.

Our research first examined the different changes occurring in the proportion of apoptotic cells. We then employed flow cytometry, and a greater number of apoptosis cells were detected upon sh-*NIFK-AS1* transfections in the HepG2 cell line (*Figure 5C,5D*).

We also examined the effect of *NIFK-AS1* knockdown on the cell cycle by flow cytometry. By determining the cell cycle distribution at a defined time point (48 h) after both sh-*NIFK-AS1* transfections, only around 40% of the cells had progressed to the G2/M phase, while 60% of the cells were still in the G0/G1 phase. For those transfected with the negative control (sh-NC), almost 73% of the cell population was found to be in the G0/G1 phase, with around 25% remaining in the G2/M phase (*Figure 5E*). This was true for both *NIFK-AS1*-specific shRNAs in HepG2 cells; reduced cell cycle progression in the G2/M phase was only observed following transfection with the more potent sh-NIFK-AS1-#2 (*Figure 5F*).

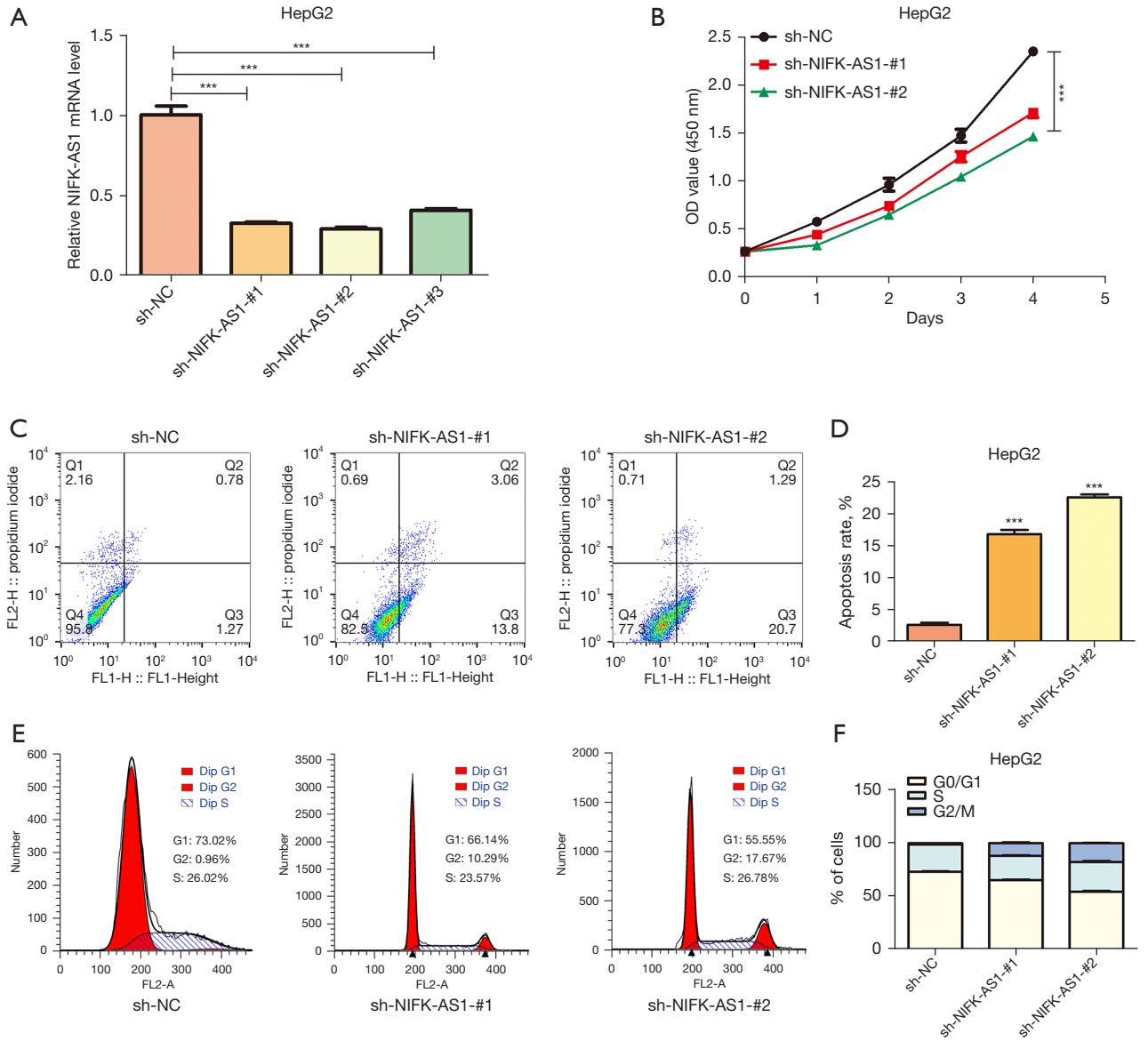

Figure 5 The results and consequences of *NIFK-AS1* gene knockdown on cell proliferation, apoptosis, and the cell cycle. (A) *NIFK-AS1* mRNA level following transfection of HepG2 cells with sh-NC or three sh-*NIFK-AS1*. (B) CCK-8 determination at the designated time point. (C) Flow cytometry was used to detect the results and consequences of *NIFK-AS1* gene knockdown on HepG2 apoptosis of cells. (D) The cell cycle distribution was analyzed by FACS, which was carried out 48 hours after transfection (n=3), (***, P<0.001). (E) Representative images of sh-NC, and sh-*NIFK-AS1* transfected HepG2 cells were analyzed in cell cycle assay. (F) Quantification of sh-NC, and sh-NIFK-AS1transfected HepG2 cells were analyzed in cell cycle assay. *NIFK-AS1*, NIFK antisense RNA 1; CCK-8, Cell Counting Kit-8; FACS, Fluorescence activated Cell Sorting; OD, optical density.

NIFK-AS1 mediates cell growth through interaction with SRSF10

We further evaluated the possible interaction between *NIFK-AS1* and *SRSF10* using bioinformatics methods. The catRAPIDomics module predicted that 120 proteins may interact with *NIFK-AS1* (Table S3) and predicted the interaction between *SRSF10* and *NIFK-AS1*. The catRAPID signature result of an algorithm module in the catRAPID server showed that the overall score of

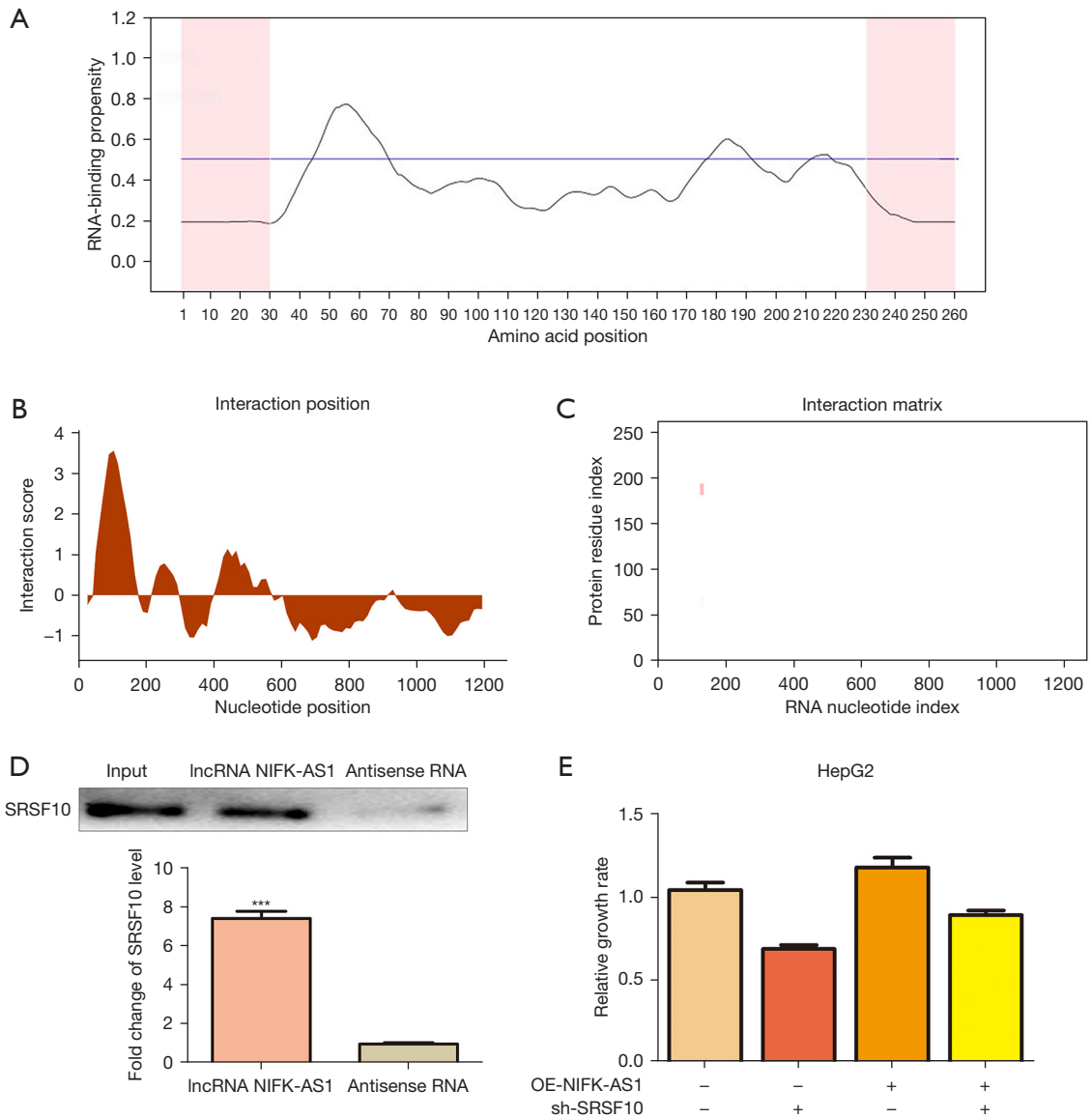

Figure 6 The bioinformatics determination and biochemical character of related proteins expressed by the *NIFK-AS1* gene. (A) The CatRAPID module prediction aimed to predict the RNA binding tendency of the *SRSF10* protein, followed by RNA binding region prediction. An interaction score with an index >0.5 was considered to demonstrate binding tendency. (B,C) The interaction spectrum and matrix between the *SRSF10* protein and the *NIFK-AS1* CatRAPID fragment module prediction. (D) The antisense RNA probe was adopted as a negative control in the precipitation of the SRSF10 protein level in NIFK-AS1 (***, P<0.001). (E) *NIFK-AS1* overexpression rescued the growth of *SRSF10* knockdown cells. *NIFK-AS1*, NIFK antisense RNA 1; CCK-8, Cell Counting Kit-8; FACS, fluorescence-activated cell sorting.

the *NIFK-AS1/SRSF10* interaction was 0.78 (*Figure 6A*). Subsequently, the catRAPID fragment was adopted through a different algorithm derived from the tendency of individual peptide interactions and nucleotide sequence fragments. This method demonstrated that 117-168 and 126-177 nucleotide positions on the *NIFK-AS1* sequence had a high tendency and possibility to connect and merge with the amino acid residues 176-227 of the high-propensity SRSF10 protein (*Figure 6B,6C*).

To confirm the *NIFK-AS1/SRSF10* interaction from a

biochemical perspective, we performed RNA pull-down to detect the interaction between *NIFK-AS1* and *SRSF10*. As shown in *Figure 6D*, compared with the antisense RNA probe set, we observed a higher protein level of biotin-labeled *SRSF10* in the *NIFK-AS1* pull-down particles. These results indicated that *NIFK-AS1* interacts with *SRSF10* in HCC cells. To further clarify and confirm the epigenetic rescue consequences of *SRSF10* on *NIFK-AS1* expression, we examined whether the overexpression of *NIFK-AS1* is sufficient to rescue the growth of SRSF10 knockdown HepG2 cells. The results showed that treatment of SRSF10 knockdown cells with *NIFK-AS1* overexpression partially rescued the growth of HepG2 cells (*Figure 6E*).

Discussion

NIFK-AS1 is an emerging cancer-related biomarker, although its relationship with tumors has been rarely reported. A previous study has confirmed that *NIFK-AS1* expression is significantly down-regulated in tamoxifen (TAM) isolated from endometrial carcinoma (EC) (17). Thus, the expression of *NIFK-AS1* is related to the development of EC. Also, *in vitro* experiments have shown that *NIFK-AS1* inhibits the migration, proliferation, and invasion of EC cells. The above actions and consequences are generally induced by an element known as estradiol 17β, which acts to limit the biochemical polarization of macrophages that looks similar to M2. In addition, the *NIFK-AS1* gene could also regulate the expression level and attributes of Notch1 by down-regulating the behavior of miR-146a. Such observations and experiments indicate that the *NIFK-AS1* gene is crucial for the regulation and adjustment of the polarization level and functional behavior of TAM in EC (17). In addition, NIFK-AS1 has previously been shown to be an effective prognostic and diagnostic biomarker and a potential therapeutic target for breast cancer (18).

In our recent study, we reported that the *NIFK-AS1* gene was significantly up-regulated in HCC tissues and cell lines. We also found that the overall survival of patients with high *NIFK-AS1* expression within HCC tumor tissues was markedly shorter than that obtained from the patients with lower *NIFK-AS1* expression levels. In other words, HCC patients that exhibited a high level of *NIFK-AS1* gene expression in their HCC-derived tumor tissues had poorer prognosis results compared to patients that did not. Also, the nomogram showed that the *NIFK-AS1* expression level could potentially exert a greater impact on the prognostic and diagnostic results of HCC patients, second only to pathological T. Through *in vitro* experiments, we found out that silencing of *NIFK-AS1* gene expression in HCC-derived cell lines could decrease cell proliferation and induce the apoptosis of cells, while at the same reducing the progression of cell cycles. These data indicate that NIFK-AS1 may be an oncogene of HCC and may contribute to the progression of HCC, and thus, could become a prognostic biomarker. Our experimental findings are consistent with previous research results.

Through the overall genome co-expression analysis results, we observed that the *NIFK-AS1* gene could potentially act as a medium in the spliceosome, homologous recombination, cell cycle, RNA transport, and DNA replication. To our knowledge, cell cycle-related molecules and related biological processes are crucial for tumor cell proliferation (19). The biological processes related to RNA transport and DNA replication are closely connected to the basic state of cells and are also closely linked with the occurrence and development of various tumors (20). We found that these differentially expressed genes (DEGs) are involved in the mitotic cell cycle process, organelle division, nuclear division, and chromosome segregation through the functional population of DEGs in patients diagnosed with HCC cancer that exhibit different levels of *NIFK-AS1* gene expression. A previous study has demonstrated that the cell cycle could potentially be treated as a targeted therapy solution for HCC, and cell cycle inhibitor scanning can be adopted as a novel therapy for advanced HCC (21).

In our study, the cell cycle distribution was determined following transfection of sh-*NIFK-AS1* into the HepG2 cell line. Compared with the sh-NC, knockdown of NIFK-AS1 has the ability to inhibit the cell cycle in the G2/M phase and affects cell cycle progression. Consistent with previous studies, our results illustrate that *NIFK-AS1* is a lncRNA that promotes cancer progression. We confirmed the lncRNA *NIFK-AS1/SRSF10* interaction through the catRAPIDomics module and RNA pull-down analysis and found that the overexpression of *NIFK-AS1* is sufficient to save the growth of HepG2 cells knocked down by *SRSF10*. These results indicate that the treatment of *SRSF10* knockdown cells with *NIFK-AS1* overexpression partially rescued the growth of HepG2 cells.

Our study showed for the first time that the NIFK-AS1 gene can potentially be adopted as a useful biomarker for the prognosis and diagnosis of HCC. Meanwhile, we managed to combine the effect survival analysis (ESA) method and nomogram analysis to determine the

practical application and importance of the *NIFK-AS1* gene for the prognosis and diagnosis of HCC patients. In addition, TCGA analysis was also adopted in our research to sequence the genome-wide RNA dataset. This study sought to identify and categorize the functional enrichment capability of the *NIFK-AS1* gene in HCC-derived tissues. The aforementioned experiment is based on the joint expression of DEGs. We adopted the functional annotations of GO and KEGG and found that lncRNAs are closely related to the cell cycle. A series of previous studies have reported that some lncRNAs were present in the occurrence of liver tumors and cancers through the cell cycle. For example, Wang *et al.* reported that cell adhesion molecule 1 AS1 (CADM1-AS1) inhibits HCC proliferation by inhibiting the AKT/glycogen synthase kinase (GSK)-3β signaling pathway, thereby up-regulating the p15, p21, and p27 expression levels, down-regulating cyclinD/E and cyclin dependent kinase 2/4/6 (CDK24/6) expression levels, and inhibiting G0/G1 to S phase transition *in vitro* and *in vivo* (21). Following knockout of lincDUSP (a potential candidate oncogene) in a colon tumor cell line derived from a patient, cell proliferation was significantly reduced, susceptibility to apoptosis increased, and early S-phase cells also increased (22). Long *et al.* found that the down-regulation of Lysyl Oxidase Like Protein 1-AS1 (LOXL1-AS1) can reduce and somewhat limit the proliferation of prostate cancer cells and cell cycle progression via Recombinant Cyclin D1 (CCND1) and miR-541-3p (23). Chen *et al.* reported that MINCR can limit and to some degree reduce the arrest of cell cycle arrest and non-small cell lung cancer (NSCLC) cell apoptosis. These methods of inhibition generally refer to c-Myc activation and consecutive effectors following activation (24).

Our research has some limitations that should be noted. Firstly, all patient data adopted in this study are from the same TCGA cohort, which represents only a small sample size. Thus, larger sample size studies are needed to confirm the conclusions of the study. Secondly, all of the data in this study comes from TCGA database and some patients' clinical data are missing, which may lead to inaccurate results. Thirdly, the molecular mechanism studies in this article are all based on bioinformatics methods such as enrichment analysis, which have only been verified *in vitro*. Therefore, the conclusions still need to be verified by *in vivo* experiments.

Despite these limitations, this study adopted the genome-wide RNA sequencing dataset and analyzed the clinical and practical importance of *NIFK-AS1* as well as its potential biochemical mechanisms in a comprehensive manner through a variety of bioinformatics analytical methods. The findings of this study could be treated as a platform that provides a theoretical basis from which the clinical applications of the *NIFK-AS1* gene in HCC can progress to a better stage.

Acknowledgments

Funding: This study was funded by a Qiqihar Academy of Medical Sciences Project Grant (No. QMSI2020L-10).

Footnote

Reporting Checklist: The authors have completed the TRIPOD and MDAR reporting checklists. Available at https://jgo.amegroups.com/article/view/10.21037/jgo-22-705/rc

Data Sharing Statement: Available at https://jgo.amegroups.com/article/view/10.21037/jgo-22-705/dss

Conflicts of Interest: All authors have completed the ICMJE uniform disclosure form (available at https://jgo.amegroups.com/article/view/10.21037/jgo-22-705/coif). The authors have no conflicts of interest to declare.

Ethical Statement: The authors are accountable for all aspects of the work in ensuring that questions related to the accuracy or integrity of any part of the work are appropriately investigated and resolved. The study was conducted in accordance with the Declaration of Helsinki (as revised in 2013) and was approved by the institutional ethics board of The Third Affiliated Hospital of Qiqihar Medical University (No. 2018LL-21). Informed consent was obtained from all participants.

References

1. Wang CI, Chu PM, Chen YL, et al. Chemotherapeutic Drug-Regulated Cytokines Might Influence Therapeutic Efficacy in HCC. Int J Mol Sci 2021;22:13627.
2. Hao X, Sun G, Zhang Y, et al. Targeting Immune Cells in the Tumor Microenvironment of HCC: New Opportunities and Challenges. Front Cell Dev Biol 2021;9:775462.
3. Wu Z, Chen W, Ouyang T, et al. Management and survival for patients with stage-I hepatocellular carcinoma: An observational study based on SEER database. Medicine (Baltimore) 2020;99:e22118.
4. Xu X, Chen J, Wei Q, et al. Clinical practice guidelines on liver transplantation for hepatocellular carcinoma in China (2018 edition). Hepatobiliary Pancreat Dis Int 2019;18:307-12.
5. Omata M, Cheng AL, Kokudo N, et al. Asia-Pacific clinical practice guidelines on the management of hepatocellular carcinoma: a 2017 update. Hepatol Int 2017;11:317-70.
6. Papoutsoglou P, Moustakas A. Long non-coding RNAs and TGF-β signaling in cancer. Cancer Sci 2020;111:2672-81.
7. Chi Y, Wang D, Wang J, et al. Long Non-Coding RNA in the Pathogenesis of Cancers. Cells 2019;8:1015.
8. Lin C, Zhang S, Wang Y, et al. Functional Role of a Novel Long Noncoding RNA TTN-AS1 in Esophageal Squamous Cell Carcinoma Progression and Metastasis. Clin Cancer Res 2018;24:486-98.
9. Wang J, Xu W, He Y, et al. LncRNA MEG3 impacts proliferation, invasion, and migration of ovarian cancer cells through regulating PTEN. Inflamm Res 2018;67:927-36.
10. Huang JL, Cao SW, Ou QS, et al. The long non-coding RNA PTTG3P promotes cell growth and metastasis via up-regulating PTTG1 and activating PI3K/AKT signaling in hepatocellular carcinoma. Mol Cancer 2018;17:93.
11. Wang J, Liu ZH, Yu LJ. Long non-coding RNA LINC00641 promotes cell growth and migration through modulating miR-378a/ZBTB20 axis in acute myeloid leukemia. Eur Rev Med Pharmacol Sci 2019;23:7498-509.
12. Qiu L, Tang Q, Li G, et al. Long non-coding RNAs as biomarkers and therapeutic targets: Recent insights into hepatocellular carcinoma. Life Sci 2017;191:273-82.
13. Xie X, Tang B, Xiao YF, et al. Long non-coding RNAs in colorectal cancer. Oncotarget 2016;7:5226-39.
14. Zhou C, Wang S, Zhou Q, et al. A Long Non-coding RNA Signature to Improve Prognostic Prediction of Pancreatic Ductal Adenocarcinoma. Front Oncol 2019;9:1160.
15. Yang J, Qi M, Fei X, et al. Long non-coding RNA XIST: a novel oncogene in multiple cancers. Mol Med 2021;27:159.
16. Das R, Feng FY, Selth LA. Long non-coding RNAs in prostate cancer: Biological and clinical implications. Mol Cell Endocrinol 2019;480:142-52.
17. Zhou YX, Zhao W, Mao LW, et al. Long non-coding RNA NIFK-AS1 inhibits M2 polarization of macrophages in endometrial cancer through targeting miR-146a. Int J Biochem Cell Biol 2018;104:25-33.
18. Zhang Y, Li Z, Chen M, et al. Identification of a New Eight-Long Noncoding RNA Molecular Signature for Breast Cancer Survival Prediction. DNA Cell Biol 2019;38:1529-39.
19. Roy D, Sheng GY, Herve S, et al. Interplay between cancer cell cycle and metabolism: Challenges, targets and therapeutic opportunities. Biomed Pharmacother 2017;89:288-96.
20. Kondo Y, Shinjo K, Katsushima K. Long non-coding RNAs as an epigenetic regulator in human cancers. Cancer Sci 2017;108:1927-33.
21. Wang F, Qi X, Li Z, et al. lncRNA CADM1-AS1 inhibits cell-cycle progression and invasion via PTEN/AKT/GSK-3β axis in hepatocellular carcinoma. Cancer Manag Res 2019;11:3813-28.
22. Forrest ME, Saiakhova A, Beard L, et al. Colon Cancer-Upregulated Long Non-Coding RNA lincDUSP Regulates Cell Cycle Genes and Potentiates Resistance to Apoptosis. Sci Rep 2018;8:7324.
23. Long B, Li N, Xu XX, et al. Long noncoding RNA LOXL1-AS1 regulates prostate cancer cell proliferation and cell cycle progression through miR-541-3p and CCND1. Biochem Biophys Res Commun 2018;505:561-8.
24. Chen S, Gu T, Lu Z, et al. Roles of MYC-targeting long non-coding RNA MINCR in cell cycle regulation and apoptosis in non-small cell lung Cancer. Respir Res 2019;20:202.

(English Language Editor: A. Kassem)

Cite this article as: Song H, Li W, Guo S, He Z, Liu S, Duo Y. A novel biomarker NIFK-AS1 promotes hepatocellular carcinoma cell cycle progression through interaction with *SRSF10*. J Gastrointest Oncol 2022;13(4):1927-1941. doi: 10.21037/jgo-22-705

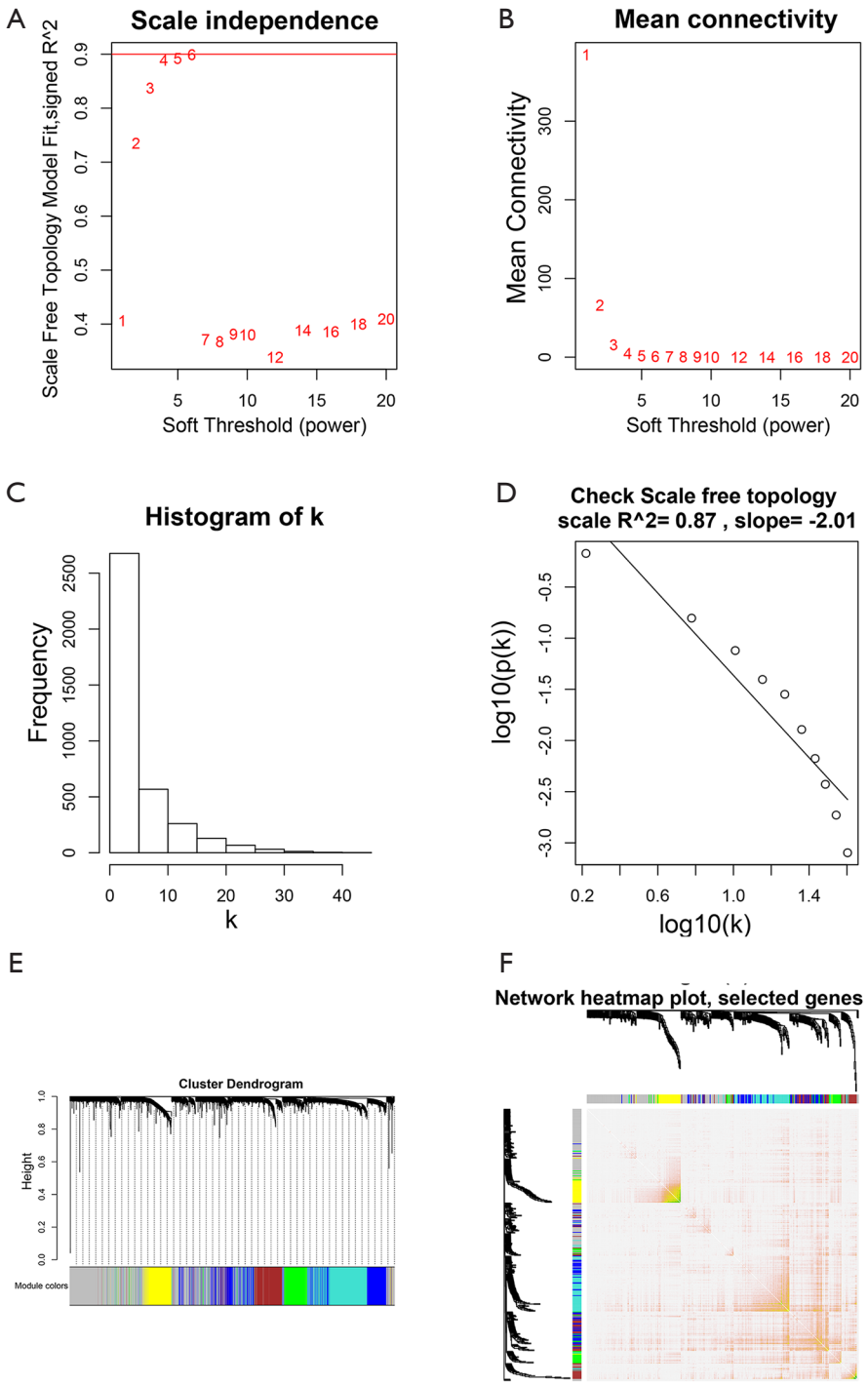

Figure S1 Weighted co-expression network construction and identification.

https://dx.doi.org/10.21037/jgo-22-705

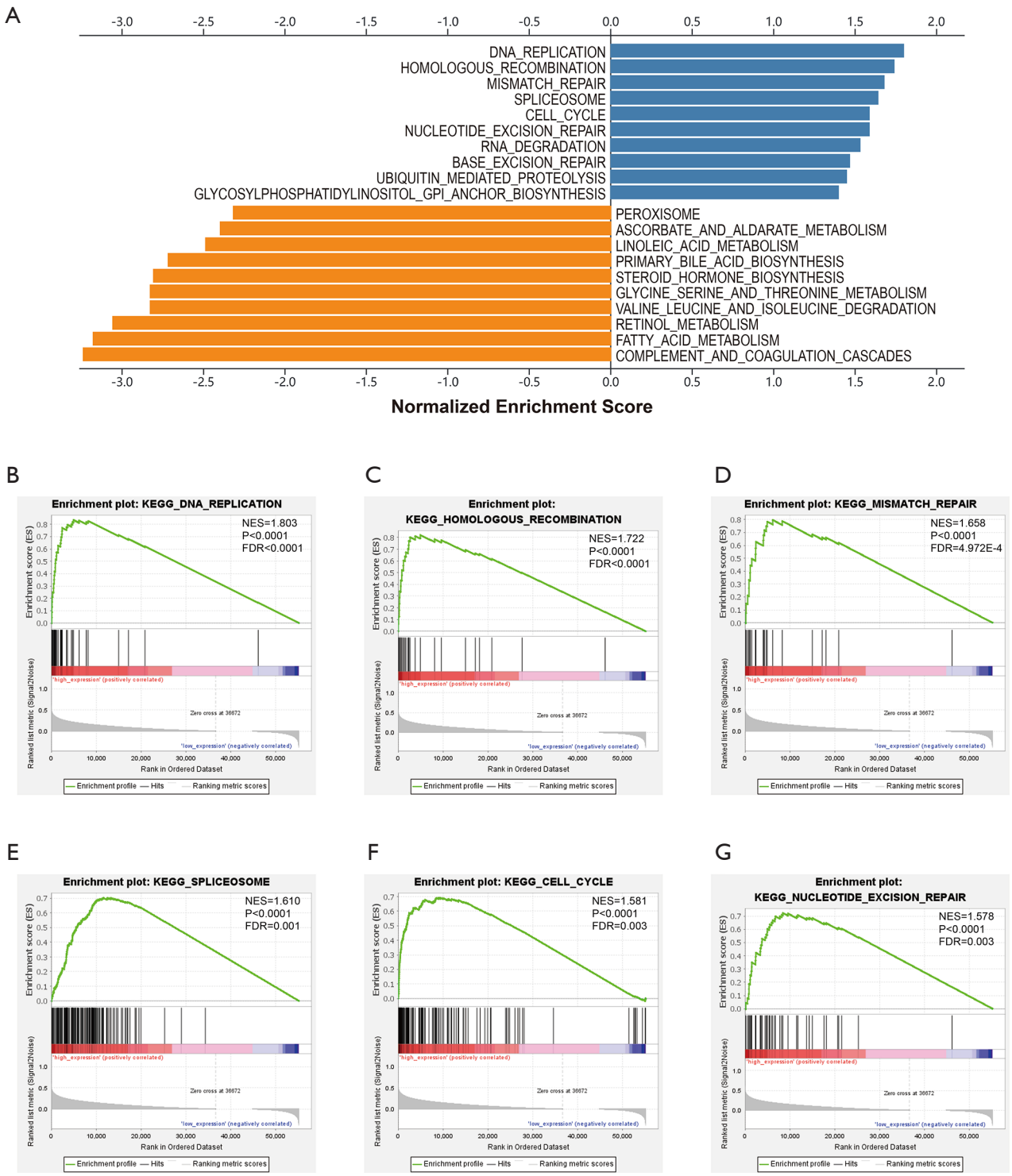

Figure S2 Gene set enrichment analysis results enriched in phenotype of high NIFK-AS1 expression group.

https://dx.doi.org/10.21037/jgo-22-705